Biosensors and Bioelectronics 87 (2017) 388–395

Contents lists available at ScienceDirect

Biosensors and Bioelectronics

journal homepage: www.elsevier.com/locate/bios

A novel label-free cell-based assay technology using biolayer interferometry

D. Verzijl [a], T. Riedl [a], P.W.H.I. Parren [a,b], A.F. Gerritsen [a,*]

[a] Genmab, Yalelaan 60, Utrecht, 3584 CM, The Netherlands
[b] Department of Immunohematology and Blood Transfusion, Leiden University Medical Center, Albinusdreef 2, Leiden, 2333 ZA, The Netherlands

ARTICLE INFO

Article history:
Received 23 June 2016
Received in revised form
26 August 2016
Accepted 27 August 2016
Available online 28 August 2016

Keywords:
Biolayer interferometry
Cell-based
Label-free
Dynamic mass redistribution
Biosensor
ForteBio Octet HTX

ABSTRACT

Biolayer interferometry (BLI) is a well-established optical label-free technique to study biomolecular interactions. Here we describe for the first time a cell-based BLI (cBLI) application that allows label-free real-time monitoring of signal transduction in living cells. Human A431 epidermoid carcinoma cells were captured onto collagen-coated biosensors and serum-starved, followed by exposure to agonistic compounds targeting various receptors, while recording the cBLI signal. Stimulation of the epidermal growth factor receptor (EGFR) with EGF, the β_2-adrenoceptor with dopamine, or the hepatocyte growth factor receptor (HGFR/c-MET) with an agonistic antibody resulted in distinct cBLI signal patterns. We show that the mechanism underlying the observed changes in cBLI signal is mediated by rearrangement of the actin cytoskeleton, a process referred to as dynamic mass redistribution (DMR). A panel of ligand-binding blocking and non-blocking anti-EGFR antibodies was used to demonstrate that this novel BLI application can be efficiently used as a label-free cellular assay for compound screening and characterization.

1. Introduction

Cellular signal transduction upon receptor stimulation is traditionally measured using classical biochemical assays, for instance by the quantification of second messenger molecules or determination of the phosphorylation status of a protein. However, a cellular response often involves activation of a complex network of signaling molecules. By focusing on a single readout other relevant signaling pathways may be overlooked. In addition, when screening orphan receptors there often is no knowledge of which signal transduction route is activated by the receptor. These challenges can be overcome by measuring an integral cellular response, instead of a single pathway. Advantages of such an integral approach are that no prior knowledge of the signal transduction cascade is required, and that responses often can be followed in time which allows evaluation of different signaling dynamics between compounds. There are commercially available label-free plate-based approaches that measure an integral outcome of cellular activation. Examples are the xCELLigence (Acea Biosciences) which measures a change in impedance upon stimulation of adherent cells over time, and the Epic (Corning) and BIND (SRU Biosystems) instruments that make use of the optical resonant waveguide grating technique.

Biolayer interferometry (BLI) is a label-free method that is commonly used to detect biomolecular interactions. In BLI the interference pattern of white light reflected from two surfaces on a disposable fiber optic-based biosensor is analyzed. The first surface on the biosensor tip consists of a layer of immobilized molecules, and the second surface is an internal reference layer. A change in the number of molecules bound to the biosensor tip causes a shift in the interference pattern that can be measured in real-time (Do et al., 2008). We developed a new BLI application that is compatible with living cells. Human A431 epidermoid carcinoma cells were captured on optical biosensors and exposed to a diverse set of agonistic compounds. This resulted in dose-dependent and compound-specific BLI signals. We show that the observed changes in BLI signal are the consequence of intracellular signaling affecting actin remodeling. Actin remodeling is thought to lead to changes in optical density by the redistribution of intracellular mass toward or away from the interface of the cell with the biosensor, a process referred to as dynamic mass redistribution (DMR) (Grundmann and Kostenis, 2015). Finally, we show that this unbiased label-free cell-based technique can easily be applied to functionally screen a panel of anti-EGFR antibodies for antagonistic properties.

* Corresponding author.
E-mail address: A.Gerritsen@genmab.com (A.F. Gerritsen).

http://dx.doi.org/10.1016/j.bios.2016.08.095

2. Materials and methods

2.1. Antibodies and compounds

The human antibodies specific to human EGFR zalutumumab and monoclonal antibodies (mAbs) 003, 005, 011 and 018 have been described previously (Bleeker et al., 2004; Dechant et al., 2008). IgG1-cMET specific for HGFR/c-MET was generated by immunizing HuMab mice (Medarex) with alternating NCI-H441 tumor cells and recombinant His-tagged extracellular domain of c-MET coupled to keyhole limpet hemocyanin (cMetECDHis-KLH). Antibody IgG1-cMET and mAbs 003, 005, 011 and 018 carried an engineered K409R mutation in the CH3 region (Labrijn et al., 2013) which does not affect binding or functional IgG1 properties. IgG1-cMET had an additional N297Q mutation (Tao and Morrison, 1989) which does not affect the antigen binding properties of IgG1-cMET. Nimotuzumab (Mateo et al., 1997), ICR62 (Modjtahedi et al., 1993), necitumumab (Lu et al., 2004), mAb 806, and IgG1-cMET were expressed in Freestyle™ HEK293-F cells (Invitrogen). Matuzumab (Murthy et al., 1987) was expressed in Expi293F™ cells (Gibco). IgG1-b12 directed against the envelope glycoprotein gp120 of human immunodeficiency virus type 1 (Roben et al., 1994) was expressed in CHOK1SV cells (Lonza). Antibodies were produced as human IgG1 with a κ light chain, purified using protein A affinity chromatography (MabSelectSuRe, GE Healthcare) and formulated in phosphate-buffered saline (B. Braun). Zalutumumab was produced by Lonza. Cetuximab (Erbitux) (Berger et al., 2011), panitumumab (Vectibix) (Yang et al., 1999) and trastuzumab (Herceptin) (Carter et al., 1992) were from Merck, Amgen and Roche respectively. Mouse anti-human EGFR IgG2a 528 (Kawamoto et al., 1983) was purchased from Calbiochem. Generation of the bispecific DuoBody molecule BsAb-cMETxb12 from the parental antibodies IgG1-cMET-F405L and IgG1-b12-K409R was performed as previously described (Labrijn et al., 2014), using an 1.3-fold excess of IgG1-b12-K409R in order to minimize the amount of residual agonistic IgG1-cMET-F405L homodimer in the DuoBody batch. The residual amount of IgG1-cMET-F405L homodimer was 0.3% as determined by cation exchange chromatography. Epidermal Growth Factor (EGF) and dopamine hydrochloride were obtained from Sigma-Aldrich.

2.2. Cell culture and capture of cells to biosensors

Amine-reactive second-generation biosensors (ForteBio) were incubated for 2 h at room temperature with a solution (0.1–1.0 mg/ml) of Collagen I, high concentration from rat tail (Corning) in water (B. Braun) followed by air-drying for at least 2 h. Human A431 cells (Deutsche Sammlung von Mikroorganismen und Zellkulturen) were cultured in RPMI 1640 (Lonza) containing 10% heat-inactivated donor bovine serum with iron, New Zealand origin (Gibco), penicillin (50 U/ml) and streptomycin (50 U/ml) (Lonza). Cells were harvested using Trypsin-EDTA (Lonza), washed with culture medium, and resuspended in undiluted 2 × Happy Cell RPMI Advanced Suspension Medium (Biocroi) to 10×10^6 cells/ml. 40 μl/well cell suspension was transferred to a 384 tilted-well plate (ForteBio). The collagen-coated biosensors were pre-wet for 10 min using 100 μl RPMI 1640 supplemented with penicillin and streptomycin in a 96 well half-area plate (Greiner Bio-One) inside an Octet HTX instrument (ForteBio), while the 384 tilted well plate was incubated at 30 °C at a shaker speed of 300 rpm. Capture of the cells to collagen-coated biosensors was then performed for 2000 s at 30 °C and a shaker speed of 300 rpm.

After capture of the cells the biosensors were transferred to serum-starvation medium (RPMI 1640 containing 0.1% serum, penicillin and streptomycin) and incubated overnight for at least 20 h in a cell culture incubator.

2.3. Cell-based biolayer interferometry

After overnight serum-starvation the collagen-coated biosensors containing cells were placed into the Octet HTX. Sample solutions containing compounds with or without inhibitors were prepared in serum-starvation medium in 384 tilted-well plates. After 10 min incubation of the sample plate at 30 °C with 300 rpm shaking, biosensors were dipped into serum-starvation medium with or without inhibitors for 1000 s in order to equilibrate. Next, the biosensors were dipped into sample solutions for 2000 s at 30 °C with 300 rpm shaking.

When indicated, the biosensors containing A431 cells were fixed with 3.7% formaldehyde (Sigma-Aldrich) in PBS for 15 min at room temperature. When indicated, the collagen-coated biosensors containing A431 cells were pretreated for 2 h in a cell culture incubator with serum-starvation medium containing the EGFR inhibitor tyrphostin AG-1478 (1 μM, Tocris), the β_2-adrenoceptor antagonist propranolol (1 μM, Tocris), the actin inhibitor cytochalasin B (10 μM, Sigma-Aldrich) or antibodies (15 μg/ml, 100 nM). Whenever inhibitors from DMSO stocks were used, the total amount of DMSO (Sigma-Aldrich) in the serum-starvation medium was kept constant at 0.05%, including solutions used for pretreatment, baseline and controls. The data traces shown in the graphs were obtained after subtraction of reference sensors exposed to serum-starvation medium with or without the appropriate inhibitors, using Data Analysis software v8.1 (ForteBio). The processed data were plotted using Prism 6 (Graphpad Software).

2.4. Cell viability

After cell capture using collagen-coated or untreated control biosensors, biosensors were incubated overnight in a cell culture incubator in serum-starvation medium containing 10% AlamarBlue (Invitrogen). The next day, fluorescence (excitation 515 nm, emission 615 nm) was determined using an EnVision Multilabel Reader (PerkinElmer). The two groups were compared with the Welch-corrected *t*-test using Prism 6.

2.5. Biosensor images

Images of the tip of the biosensor were taken while the biosensor was kept vertically above a 96 well half-area plate with the biosensor tip submerged in medium, using a Zeiss Axiovert 40 C inverted microscope in combination with a Canon G10 PowerShot digital camera.

3. Results

3.1. Capture of living cells to biosensors

In a typical biolayer interferometry (BLI) experiment using the Octet HTX platform, biosensors coated with a biocompatible matrix are used to interrogate 96- or 384-well plates by dipping the biosensors in the sample solution. This design implies that when adherent cells are to be captured from a cell suspension to the biosensor surface, the cells need to adhere to the bottom of the biosensor. Therefore the biosensors need to be coated with an agent that allows fast and firm attachment of living cells. To this end, the biosensors were coated with the extracellular matrix protein collagen type I.

The adherent human epidermoid carcinoma cell line A431 was suspended in 2 × Happy Cell Advanced Suspension Medium. The composition of Happy Cell Advanced Suspension Medium is designed to keep cells floating in suspension and was originally developed for 3D culture of cells. This property was exploited to

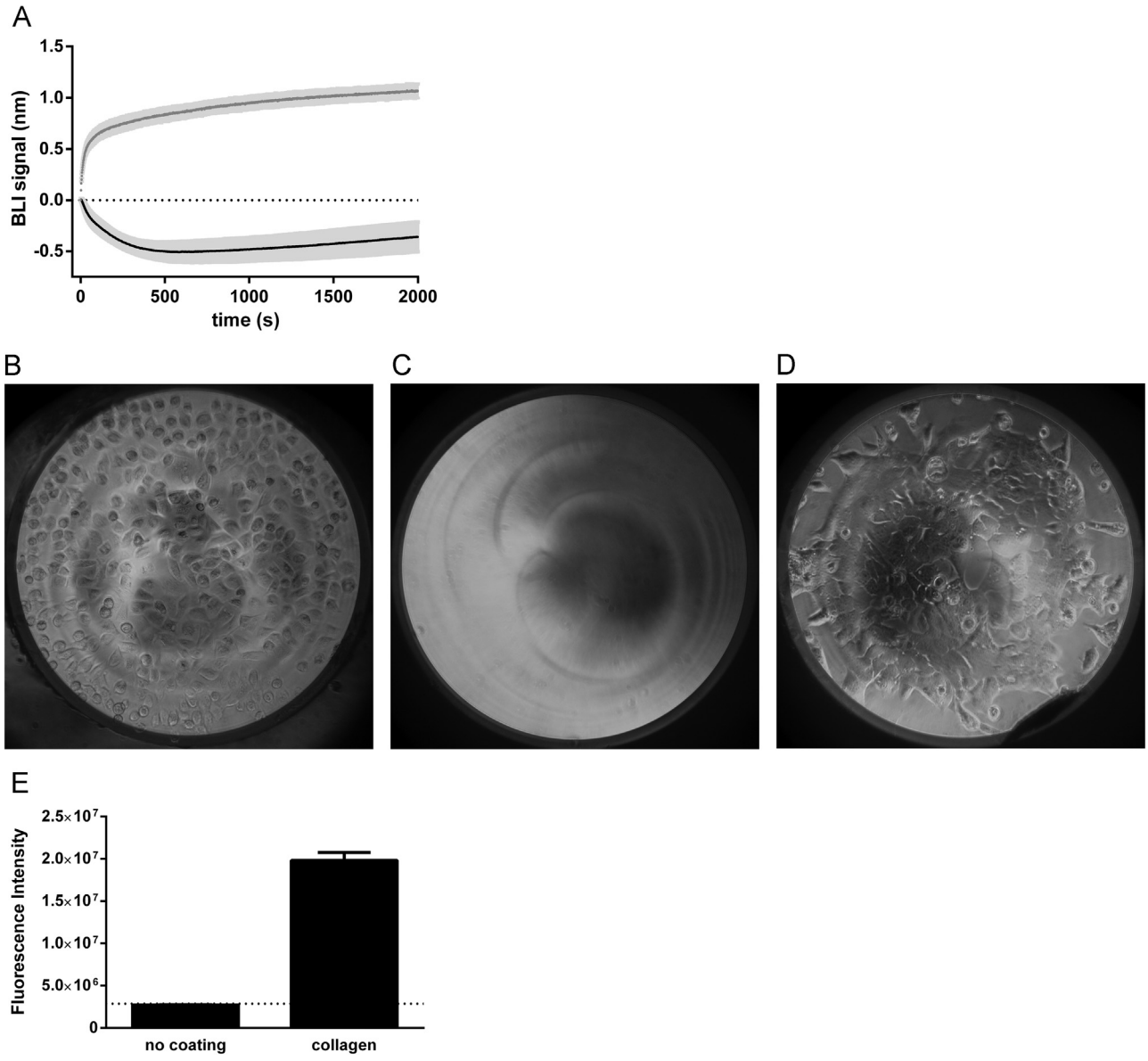

Fig. 1. Capture and viability of A431 cells. (A) Collagen-coated (black) or non-coated control (grey) biosensors were dipped in a suspension of cells and the BLI signal was recorded for 2000 s. The average signal including standard deviation (grey shading) of 92 collagen-coated biosensors and 4 non-coated biosensors from a representative experiment is shown. Pictures of a collagen-coated **(B)** and non-coated control **(C)** biosensor tip were taken directly after the cell capture experiment. The diameter of a biosensor tip is 0.6 mm. **(D)** A collagen-coated biosensor tip was incubated overnight under low serum conditions and a picture was taken the next day. **(E)** Viability of A431 cells captured on 4 collagen-coated biosensors after overnight serum-starvation was determined using AlamarBlue and compared with 4 non-coated biosensors or wells containing no biosensors (dashed line). Representative experiments are shown.

prevent A431 cells from sedimenting to the bottom of the wells, allowing cell adhesion onto the biosensors.

During incubation of the biosensors with the cell suspension, a reproducible BLI signal was recorded (Fig. 1A). Capture of cells on collagen-coated biosensors resulted in a negative BLI signal, while non-collagen-coated control biosensors showed a positive signal when dipped in the cell suspension. It was not unexpected that cell capture resulted in a negative BLI signal, since binding of large particles to the optical biosensors can result in a negative nm shift rather than a positive nm shift.

Brightfield imaging of the biosensors directly after cell capture revealed that cells adhered only to the biosensor surface after collagen-coating (Fig. 1B) but not to non-coated sensors (Fig. 1C). After overnight incubation in serum-starvation medium the cells had acquired a stretched morphology (Fig. 1D).

The viability of cells on collagen-coated biosensors was addressed by an AlamarBlue cell viability assay. A significant increase in fluorescent AlamarBlue signal was observed for the collagen-coated biosensors with cells, versus non-coated control biosensors yielding only background signal intensity (P value < 0.0001, Fig. 1E). This shows that A431 cells on collagen-coated biosensors are viable after capture and 24 h serum-starvation.

3.2. Agonist-induced cell-based biolayer interferometry

A431 cells express high levels of the epidermal growth factor receptor (EGFR) (Fang et al., 2005). EGFR is a single transmembrane receptor tyrosine kinase which is activated upon binding of its ligand EGF. EGF is a soluble protein with a molecular weight of approximately 6 kDa, which induces cellular proliferation, differentiation, and survival through EGFR.

A431 cells captured on collagen-coated biosensors were exposed to different concentrations of EGF while recording the cell-based BLI (cBLI) signal. A time- and dose-dependent positive cBLI

signal was obtained (Fig. 2A). The cBLI signal reached a maximum after approximately 1000 s. When the signal at 1000 s was plotted against the EGF concentration, a dose-response relationship was observed with an average EC_{50} value of 2.2 ± 1.8 nM (Fig. 2B).

A431 cells also endogenously express the β_2-adrenoceptor, a member of the G protein-coupled receptor (GPCR) family (Fang

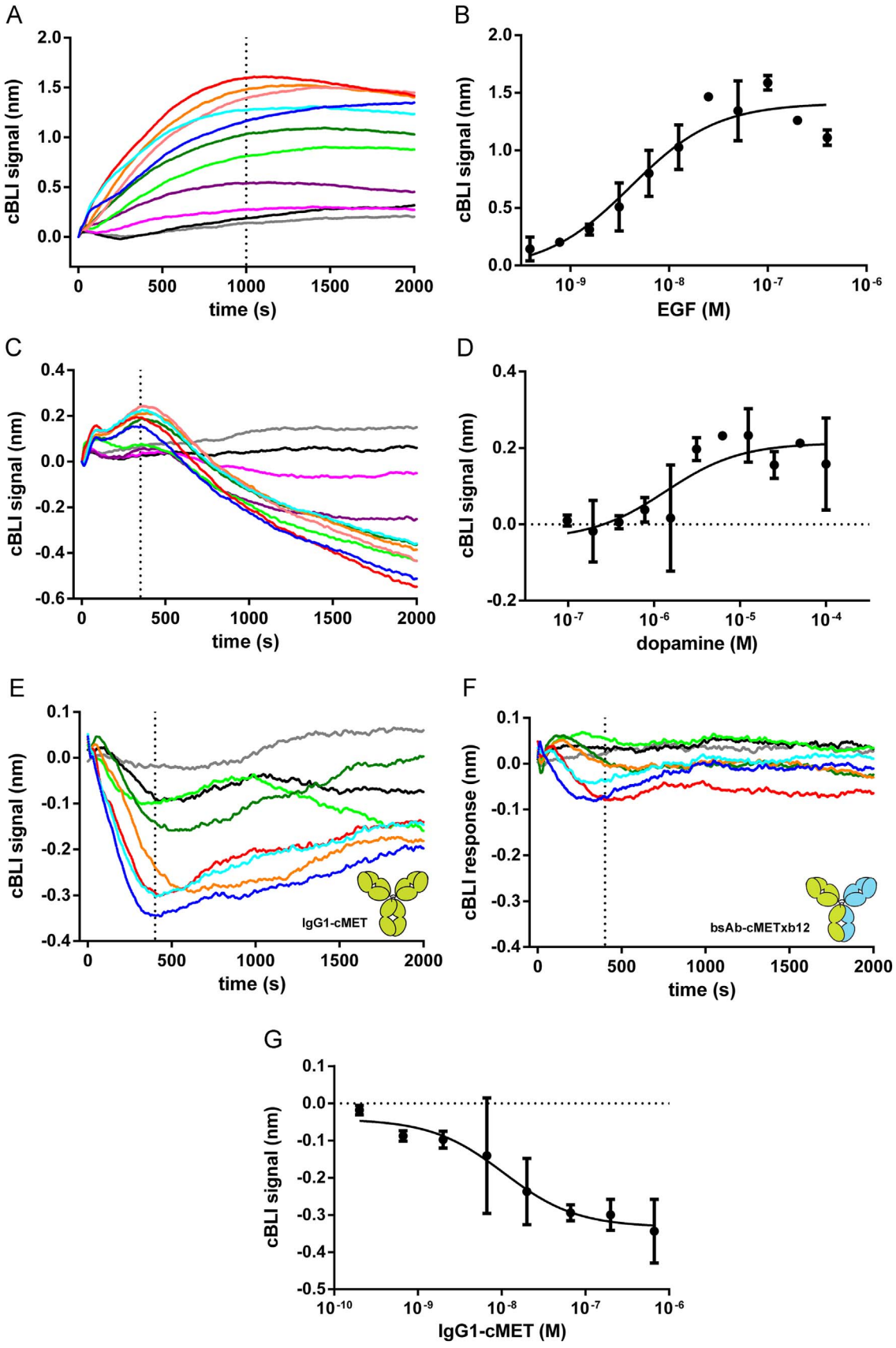

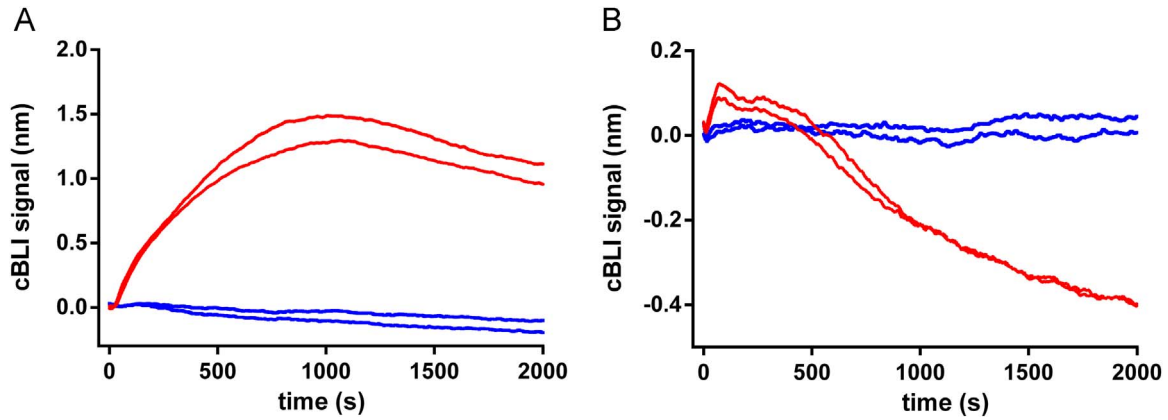

Fig. 3. Inhibition of receptor activation abrogates cBLI signal. (A) A431 cells were pretreated for 2 h with the EGFR tyrosine kinase inhibitor AG-1478 (1 μM, blue traces) or control medium (red traces) and the cBLI signal induced by EGF (100 nM) was determined. **(B)** Cells were pretreated for 2 h with the β_2-adrenoceptor antagonist propranolol (1 μM, blue traces) or control medium (red traces) and the cBLI signal induced by dopamine (100 μM) was determined. Each graph shows data from a representative experiment performed with duplicate biosensors, and each experiment was repeated three times.

and Ferrie, 2008). The β_2-adrenoceptor is activated by low molecular weight compounds such as adrenaline and dopamine. Exposure of cells captured on collagen-coated biosensors to dopamine (molecular weight 153 Da) resulted in a cBLI signal distinct from the one observed for EGF exposure. The dopamine-induced cBLI signal consisted of two phases (Fig. 2C): a positive signal which peaked after approximately 350 s, followed by a negative signal. When the cBLI signal at 350 s was plotted against the concentration of dopamine, an average EC_{50} of 2.3 ± 2.1 μM was observed (Fig. 2D).

The hepatocyte growth factor receptor (HGFR), also called c-MET, is another receptor tyrosine kinase that is expressed on A431 cells. c-MET is essential in wound healing, embryonic development and organogenesis, and plays an important role in the development of many human cancers. Inhibition of the interaction between c-MET and its ligand HGF, for example with monoclonal antibodies, may be of therapeutic value. However, many bivalent antibodies directed against c-MET have unwanted intrinsic agonistic activity because they induce homodimerization by cross-linking two c-MET receptors, which results in self-activation of c-MET (Prat et al., 1998). We studied the effect of the bivalent antibody IgG1-cMET on A431 cells that were captured on collagen-coated biosensors. IgG1-cMET (molecular weight approximately 150 kDa) dose-dependently induced a negative cBLI signal which reached a minimum around 400 s (Fig. 2E). The shape of the cBLI signal observed with IgG1-cMET was distinct from the signals obtained with EGF or dopamine and was specific to IgG1-cMET, as no significant changes in the cBLI signal were observed in the presence of the negative control antibody IgG1-b12. IgG1-b12 is directed against a target that is not expressed on A431 cells, i.e. the human immunodeficiency virus-1 envelope protein gp120.

In order to further evidence the specificity of the cBLI signal towards antibody-induced homodimerization of c-MET, we tested a bispecific functionally monovalent version of IgG1-cMET, based on the DuoBody® format (Labrijn et al., 2014). The bispecific antibody was constructed with one Fab-arm from IgG1-cMET while the other Fab-arm was from the negative control antibody IgG1-b12. The resulting bispecific antibody, designated BsAb-cMETxb12, is functionally monovalent and thus unable to cross-link two c-MET receptors. Exposure of A431 cells to functionally monovalent BsAb-cMETxb12 significantly reduced the observed cBLI signal (Fig. 2F). This suggests that the parental bivalent IgG-cMET antibody indeed induces a cBLI signal by cross-linking and homodimerization of c-MET. At the highest concentrations tested (10–100 μg/ml) we observed a minimal residual cBLI signal to functionally monovalent BsAb-cMETxb12. We speculate that these small cBLI signals are due to the presence of trace amounts (0.3%) of bivalent IgG1-cMET in the BsAb-cMETxb12 DuoBody preparation.

The cBLI signals induced by the bivalent IgG1-cMET at 400 s were plotted against the antibody concentration. An average EC_{50} of 9.4 ± 0.4 nM, corresponding to approximately 1.5 μg/ml, was obtained for IgG1-cMET (Fig. 2F).

3.3. Inhibition of receptor activation abrogates cBLI signal

We hypothesized that the observed cBLI signals were the result of agonist-induced intracellular signaling and not a direct binding event of the compounds to their cognate receptors. In order to test this hypothesis, A431 cells were pretreated with the EGFR tyrosine kinase inhibitor tyrphostin AG-1478. AG-1478 effectively inactivates the kinase domain of EGFR and thereby inhibits EGFR-mediated signaling. Treatment of cells with AG-1478 completely inhibited the cBLI signals induced by EGF (Fig. 3A). This indicates that EGFR-mediated signal transduction causes the EGF-induced cBLI signal.

Fig. 2. Agonist-induced cell-based biolayer interferometry. (A) A431 cells were exposed to the following concentrations of EGF: 400 nM (blue); 200 nM (light blue); 100 nM (red); 50 nM (light red); 25 nM (orange); 12.5 nM (dark green); 6.25 nM (light green); 3.1 nM (purple); 1.6 nM (pink); 0.8 nM (black) and 0.4 nM (grey). Each curve represents the average of two biosensors. The dotted line at 1000 s indicates the data points used for Fig. B **(B)** The EGF-induced cBLI signal at 1000 s was plotted against the EGF concentration using a logarithmic scale. Each data point represents the average of two duplicates with standard deviation. **(C)** Cells were exposed to the following concentrations of dopamine: 100 μM (blue); 50 μM (light blue); 25 μM (red); 12.5 μM (light red); 6.25 μM (orange); 3.1 μM (dark green); 1.6 μM (light green); 800 nM (purple); 400 nM (pink); 200 nM (black) and 100 nM (grey). Each curve represents the average of two biosensors. The dotted line at 350 s indicates the data points used for Fig. D **(D)** The dopamine-induced cBLI signal at 350 s was plotted against the dopamine concentration. Each data point represents the average of two duplicates with standard deviation. **(E and F)** Cells were exposed to the following concentrations of IgG1-cMET **(E)** or BsAb-cMETxb12 **(F)**: 100 μg/ml (blue); 30 μg/ml (light blue); 10 μg/ml (red); 3.0 μg/ml (orange); 1.0 μg/ml (dark green); 0.3 μg/ml (light green); 100 ng/ml (black) and 30 ng/ml (grey). Each curve represents the average of two duplicate biosensors. The dotted line at 400 s indicates the data points used for G. Schematic representations of bivalent IgG1-cMET (green) and the functionally monovalent DuoBody molecule BsAb-cMETxb12 (green and blue) are shown in E and F respectively. **(G)** IgG1-cMET-induced cBLI signals at 400 s were plotted against the antibody concentration. Each data point represents the average of two duplicates with standard deviation. Each graph shows data from a representative experiment and each experiment was repeated three times, except for the *anti*-cMET experiment which was repeated two times.

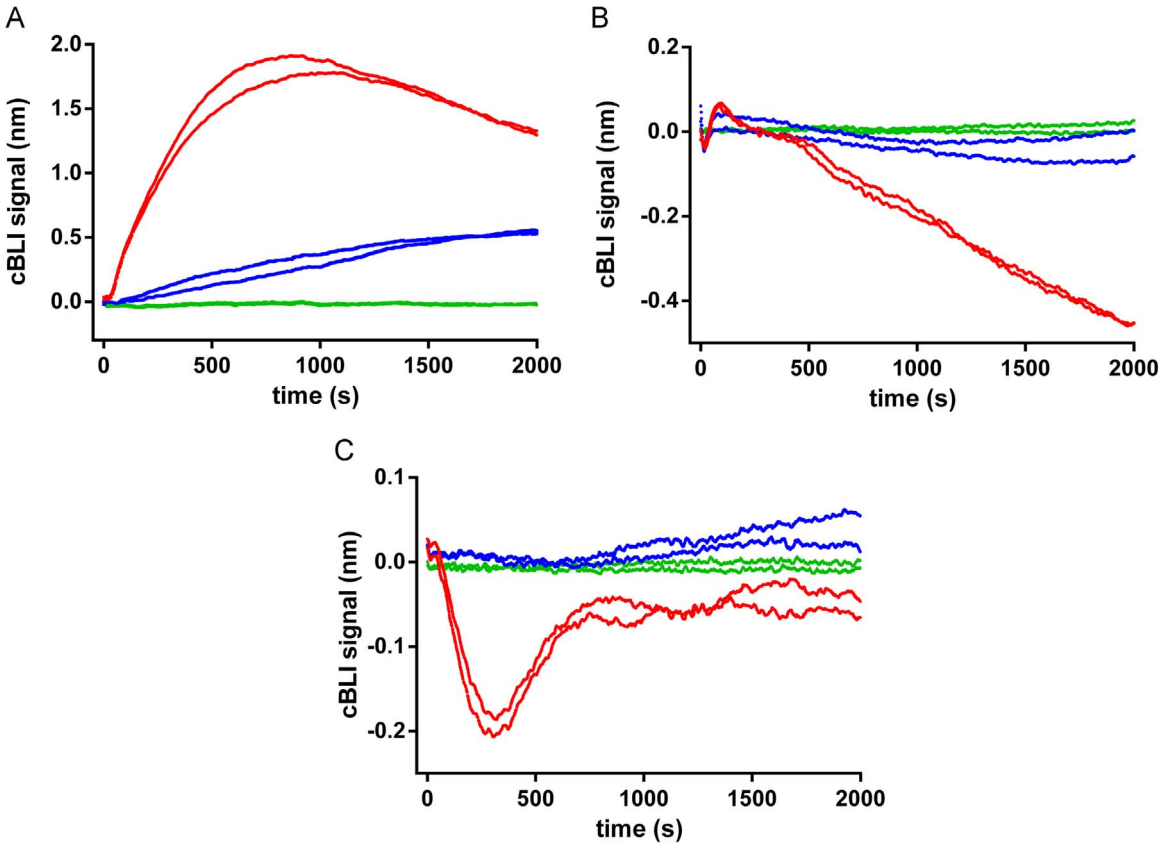

Fig. 4. Dynamic Mass Redistribution as mechanism of action. A431 cells were fixed with formaldehyde (green traces) or pretreated for 2 h with control medium (red traces) or the actin polymerization inhibitor cytochalasin B (10 μM, blue traces) and the cBLI signal induced by **(A)** EGF (100 nM), **(B)** dopamine (100 μM) or **(C)** IgG1-cMET (10 μg/ml, 67 nM) was determined. Each graph shows data from a representative experiment performed with duplicate biosensors which was repeated three times.

Next, the effect of blocking the β_2-adrenoceptor on the dopamine-mediated cBLI signal was tested. A431 cells were pre-incubated with the β_2-adrenoceptor antagonist propranolol and the dopamine response was determined in the presence of propranolol. The β_2-adrenoceptor-mediated cBLI signal induced by the agonist dopamine was completely inhibited by the antagonist propranolol (Fig. 3B). Together, these data indicate that agonist-mediated signal transduction is important in cBLI.

3.4. Dynamic mass redistribution underlies cBLI signal

In established optical label-free cell-based techniques such as resonant waveguide grating, intracellular dynamic mass redistribution (DMR) has been proposed to underlie the observed shifts in reflected wavelength (Grundmann and Kostenis, 2015). Stimulation of a cell frequently induces actin remodeling. This results in a change in optical density at the biosensor-cell interface through redistribution of intracellular mass towards or away from the biosensor surface. The actin cytoskeleton plays an important role in this process (Grundmann and Kostenis, 2015). We tested this hypothesis by interfering with actin remodeling by either chemical fixation or inhibiting actin polymerization with the low molecular weight compound cytochalasin B. In the first approach, A431 cells were captured on collagen-coated biosensors and fixed with formaldehyde. Formaldehyde fixation randomly cross-links cellular proteins and therefore prevents morphological rearrangements. Fixation of the cells prior to stimulation with EGF completely abrogated the EGFR-mediated cBLI signal (Fig. 4A). Likewise, when cells were fixed with formaldehyde both the dopamine-induced response through the β_2-adrenoceptor (Fig. 4B) as well as the c-MET-mediated cBLI signal induced by the IgG1-cMET antibody (Fig. 4C) were fully abolished. To further strengthen our finding that actin remodeling causes cBLI we treated cells with the actin polymerization inhibitor cytochalasin B. Pretreatment of cells with cytochalasin B inhibited the cBLI signals induced by EGF (Fig. 4A), dopamine (Fig. 4B), and the antibody IgG1-cMET (Fig. 4C). Together, these data strongly indicate that the cBLI signals obtained with these agonistic molecules are due to a signaling cascade that leads to DMR and morphological rearrangements.

3.5. Screening for antibodies that inhibit EGFR activation

We next investigated whether the cBLI technique may have applications in antibody discovery screening campaigns. Having shown that the EGFR tyrosine kinase inhibitor AG-1478 completely abolishes cBLI signals on cells exposed to EGF, we postulated that also antibodies that block the binding of EGF to EGFR or inhibit EGFR signaling could be identified by cBLI. To test this, serum-starved A431 cells on collagen-coated biosensors were incubated for 2 h with 100 nM of the EGF-blocking antibody cetuximab (Berger et al., 2011) or mAb 011 which has been reported to partially block EGF binding (Dechant et al., 2008). Subsequently, the cBLI signal induced by EGF (100 nM) was determined in the presence or absence of these antibodies. Cetuximab completely inhibited the EGF response, while incubation with mAb 011 resulted in partial inhibition (Fig. 5A). Incubation of cells with cetuximab or mAb 011 alone had no effect (data not shown). This result demonstrates that cBLI can help to discriminate between the agonist-blocking properties of antibodies.

We applied this setup to a panel of antibodies directed against EGFR to screen for their ability to inhibit EGF-induced signaling. Incubation of A431 cells with anti-EGFR antibodies in the absence

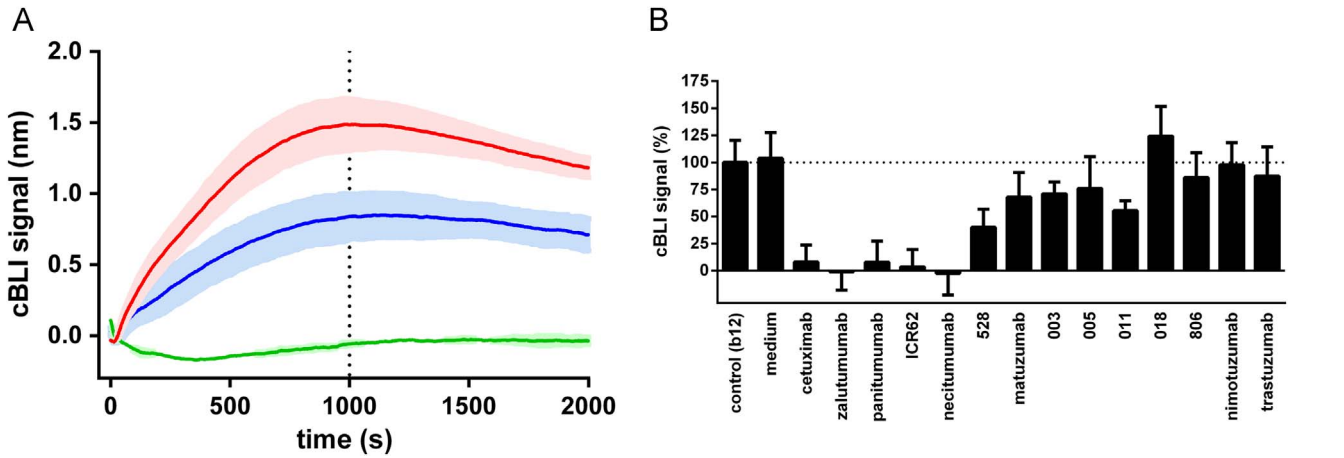

Fig. 5. Inhibition of EGF response by anti-EGFR antibodies. A431 cells were pretreated for 2 h with antibody (15 μg/ml, 100 nM) and the cBLI signal induced by EGF (100 nM) in the presence of antibody (100 nM) was recorded. **(A)** The traces represent the average with standard deviation of 4 biosensors treated with EGF only (red trace), 2 biosensors treated with cetuximab + EGF (green trace) and 2 biosensors incubated with mAb 011+ EGF (blue trace). The dotted line indicates the 1000 s time point used for the data in Fig. B. Data from a representative experiment is shown that was repeated three times. **(B)** The normalized EGF (100 nM) response at 1000 s in the presence of indicated antibodies (15 μg/ml, 100 nM) is shown. The EGF response in the presence of the negative control antibody IgG1-b12 was set as 100% and was comparable to the EGF response in the absence of antibody (medium only). The average data including standard deviation from three independent experiments performed with duplicate biosensors per antibody is shown.

of EGF had no effect (data not shown). Anti-EGFR antibodies with previously described ligand-blocking properties such as cetuximab (Berger et al., 2011), zalutumumab (Bleeker et al., 2004; Dechant et al., 2008), panitumumab (Dechant et al., 2008; Yang et al., 1999), ICR62 (Modjtahedi et al., 1993) and necitumumab (Lu et al., 2004) completely blocked the EGF response as recorded by the cBLI signal after 1000 s (Fig. 5B). The antibodies 528 (Kawamoto et al., 1983), matuzumab (Murthy et al., 1987), mAbs 003, 005 and 011 (Dechant et al., 2008) showed partial inhibition of the EGF response. Although matuzumab was reported to block EGF binding to EGFR (Murthy et al., 1987), its inhibition of the EGF response was relatively modest. This may be explained by the fact that matuzumab does not directly block access of EGF to its binding site on EGFR like cetuximab, but rather non-competitively and sterically blocks the EGFR domain-rearrangement required for high-affinity ligand binding and receptor dimerization (Schmiedel et al., 2008). As expected, mAb 018 which does not block EGF binding to EGFR (Dechant et al., 2008) and the negative control antibody trastuzumab directed against the related HER2 receptor did not inhibit the EGF-mediated cBLI signal. Similarly, mAb 806, which preferentially recognizes an EGFR variant expressed on tumor cells (Johns et al., 2002), did not block the EGF response. Also nimotuzumab was unable to block the EGF response at the used concentration, although it has been reported as a ligand-blocking antibody (Mateo et al., 1997). Indeed, in previous studies it was shown that 10- to 20-fold higher concentrations of nimotuzumab are needed to achieve full EGFR signaling blockage when compared to cetuximab, likely due to its lower affinity for EGFR (Berger et al., 2011). The results obtained with this comprehensive anti-EGFR panel indicate that this novel label-free assay technique can be successfully applied to screening for ligand-inhibiting properties of antibodies.

4. Discussion

In this report we show for the first time the applicability of biolayer interferometry (BLI) to detect changes in living cells in response to drug treatment. The BLI signals that we obtained during the capture of A431 cells to collagen-coated biosensors (Fig. 1A) are most likely the result of direct binding of the cell to the biosensor, resulting in an increase in thickness on the biosensor surface. In contrast, the cell-based BLI (cBLI) signals obtained by stimulation of cells with agonists are the result of intracellular signaling leading to dynamic mass redistribution (DMR), rather than direct binding of the agonist to the cell.

It is likely that the large size of the A431 cells prevents the detection of direct binding of compounds to the cell, which needs to take place close to the biosensor surface in order to result in a BLI signal. This is for instance exemplified by the experiment where the EGF-mediated cBLI signal is completely blocked with the EGFR tyrosine kinase inhibitor AG-1478 (Fig. 3A). When binding of EGF to EGFR expressed on the A431 cells would contribute to the observed cBLI signal, the direct binding of EGF (6 kDa) to the cells would still be recorded even though signaling is inhibited by AG-1478. Similarly, the direct binding of proteins such as EGF or the IgG1-cMET antibody (150 kDa) to formaldehyde-fixed or cytochalasin B-treated cells should result in a BLI signal when direct binding events are contributing to the cBLI signal (Fig. 4A and C).

Besides the use of collagen-coated biosensors to capture A431 cells, we have used lectins to capture cells during assay development. Lectins are proteins that bind to the sugar moieties of glycoproteins that are expressed on the cell membrane. We successfully used the lectins concanavalin A and wheat germ agglutinin to capture A431 cells, human AU565 breast carcinoma cells and the human B lymphocyte suspension cell line Raji to biosensors (Supplementary Fig. S1A-H). In addition, cells have been captured using biosensors coated with antibodies directed against cell surface-expressed targets (Supplementary Fig. S1I-K). We decided to continue our studies with collagen as a generic capture method because collagen-coating of biosensors resulted in a proper adherent morphology of the A431 cells (Fig. 1D) that contributes to an efficient interaction of the cells with the biosensor surface, which is needed for a DMR signal.

cBLI can be used to study a variety of extracellular stimuli that result in DMR without prior knowledge of the intracellular signal transduction pathways that are involved, both for agonist and antagonist characterization. Structurally and functionally diverse agonists such as the growth factor EGF, the low molecular weight agonist dopamine and a c-MET antibody elicited specific and characteristic cBLI signatures (Fig. 2). This suggests that cBLI can differentiate between different kinds of activation mechanisms. We have even noticed subtle differences in the cBLI fingerprint of

dopamine and structurally related analogs such as pindolol, alprenolol and tyramine, suggestive of ligand-directed functional selectivity (data not shown). Similar observations between dopamine and its analogs have been made by others using resonant waveguide grating (RWG), an established label-free cell-based optical biosensor technique (Fang and Ferrie, 2008). The EC_{50} for dopamine determined here using cBLI (2.3 μM) was very close to the EC_{50} generated with RWG (1 0.1 μM) (Fang and Ferrie, 2008). Also the EC_{50} value for EGF stimulation obtained with cBLI (2.2 nM) correlates very well with a study in A431 cells using RWG (K_d of 1.45 nM) (Fang et al., 2005). This implies that the integral cellular response obtained using cBLI relates well with other holistic approaches.

The inhibitor cytochalasin B was used in order to show that actin is involved in agonist-induced cBLI signals. Cytochalasin B only partially inhibited the response induced by EGF (Fig. 4A). This suggests that besides rearrangement of the actin cytoskeleton, there may be additional mechanisms involved that lead to DMR or morphological changes, resulting in a cBLI signal. We speculate that cBLI may not be limited to actin-mediated DMR responses, but may be useful in detecting other cellular changes as well, including for instance cell detachment, cell death, cell-cell interactions, membrane blebbing or degranulation.

A diverse panel of anti-EGFR antibodies was successfully screened in order to demonstrate the suitability of cBLI assay in drug screening campaigns. Moreover, the results obtained with the low molecular weight antagonist propranolol and the agonist dopamine show that such a screening is not limited to antibodies (Fig. 3B).

Summarizing, we have developed a label-free, real-time, cell-based assay that we named cell-based biolayer interferometry (cBLI), which can be applied in drug screening campaigns. This novel assay shows that BLI is a versatile technique that besides its well established use for detection of biomolecular interactions can be used to detect effects of agonistic compounds on living cells.

Declaration of interest

All authors are Genmab employees and own Genmab warrants and/or stock. A.F. Gerritsen is member of the Scientific Advisory Board of Pall Biopharmaceuticals.

Appendix A. Supplementary material

Supplementary data associated with this article can be found in the online version at http://dx.doi.org/10.1016/j.bios.2016.08.095.

References

Berger, C., Krengel, U., Stang, E., Moreno, E., Madshus, I.H., 2011. J. Immunother. 34, 550–555.
Bleeker, W.K., Lammerts van Bueren, J.J., van Ojik, H.H., Gerritsen, A.F., Pluyter, M., Houtkamp, M., Halk, E., Goldstein, J., Schuurman, J., van Dijk, M.A., van de Winkel, J.G., Parren, P.W., 2004. J. Immunol. 173, 4699–4707.
Carter, P., Presta, L., Gorman, C.M., Ridgway, J.B., Henner, D., Wong, W.L., Rowland, A.M., Kotts, C., Carver, M.E., Shepard, H.M., 1992. Proc. Natl. Acad. Sci. USA. 89, 4285–4289.
Dechant, M., Weisner, W., Berger, S., Peipp, M., Beyer, T., Schneider-Merck, T., Lammerts van Bueren, J.J., Bleeker, W.K., Parren, P.W., van de Winkel, J.G., Valerius, T., 2008. Cancer Res. 68, 4998–5003.
Do, T., Ho, F., Heidecker, B., Witte, K., Chang, L., Lerner, L., 2008. Protein Expr. Purif. 60, 147–150.
Fang, Y., Ferrie, A.M., 2008. FEBS Lett. 582, 558–564.
Fang, Y., Ferrie, A.M., Fontaine, N.H., Yuen, P.K., 2005. Anal. Chem. 77, 5720–5725.
Grundmann, M., Kostenis, E., 2015. Methods Mol. Biol. 1272, 199–213.
Johns, T.G., Stockert, E., Ritter, G., Jungbluth, A.A., Huang, H.J., Cavenee, W.K., Smyth, F.E., Hall, C.M., Watson, N., Nice, E.C., Gullick, W.J., Old, L.J., Burgess, A.W., Scott, A.M., 2002. Int. J. Cancer 98, 398–408.
Kawamoto, T., Sato, J.D., Le, A., Polikoff, J., Sato, G.H., Mendelsohn, J., 1983. Proc. Natl. Acad. Sci. USA 80, 1337–1341.
Labrijn, A.F., Meesters, J.I., Priem, P., de Jong, R.N., van den Bremer, E.T., van Kampen, M.D., Gerritsen, A.F., Schuurman, J., Parren, P.W., 2014. Nat. Protoc. 9, 2450–2463.
Labrijn, A.F., Meesters, J.I., de Goeij, B.E., van den Bremer, E.T., Neijssen, J., van Kampen, M.D., Strumane, K., Verploegen, S., Kundu, A., Gramer, M.J., van Berkel, P.H., van de Winkel, J.G., Schuurman, J., Parren, P.W., 2013. Proc. Natl. Acad. Sci. USA 110, 5145–5150.
Lu, D., Zhang, H., Ludwig, D., Persaud, A., Jimenez, X., Burtrum, D., Balderes, P., Liu, M., Bohlen, P., Witte, L., Zhu, Z., 2004. J. Biol. Chem. 279, 2856–2865.
Mateo, C., Moreno, E., Amour, K., Lombardero, J., Harris, W., Perez, R., 1997. Immunotechnology 3, 71–81.
Modjtahedi, H., Styles, J.M., Dean, C.J., 1993. Br. J. Cancer 67, 247–253.
Murthy, U., Basu, A., Rodeck, U., Herlyn, M., Ross, A.H., Das, M., 1987. Arch. Biochem. Biophys. 252, 549–560.
Prat, M., Crepaldi, T., Pennacchietti, S., Bussolino, F., Comoglio, P.M., 1998. J. Cell Sci. 111, 237–247.
Roben, P., Moore, J.P., Thali, M., Sodroski, J., Barbas, C.Fr, Burton, D.R., 1994. J. Virol. 68, 4821–4828.
Schmiedel, J., Blaukat, A., Li, S., Knochel, T., Ferguson, K.M., 2008. Cancer Cell 13, 365–373.
Tao, M.H., Morrison, S.L., 1989. J. Immunol. 143, 2595–2601.
Yang, X.D., Jia, X.C., Corvalan, J.R., Wang, P., Davis, C.G., Jakobovits, A., 1999. Cancer Res. 59, 1236–1243.